ChemMedChem

Research Article
doi.org/10.1002/cmdc.202400648

Chemistry Europe
European Chemical Societies Publishing

www.chemmedchem.org

Dual Centrifugation-Based Screening for pH-Responsive Liposomes

Lukas Gleue[+],[a] Barbara Graefen[+],[b] Matthias Voigt[+],[a, g] Jonathan Schupp[+],[b, h, i] Dirk Schneider,[c] Michael Fichter,[b, d, e] Michael Kuske,[b, e, j] Volker Mailaender,[b, d, e] Andrea Tuettenberg,*[b, f] and Mark Helm*[a]

In liposomal drug delivery development, the delicate balance of membrane stability is a major challenge to prevent leakage (during shelf-life and blood circulation), and to ensure efficient payload release at the therapeutic destination. Our composite screening approach uses the processing by dual centrifugation technique to speed up the identification of *de novo* formulations of intermediate membrane stability. By screening binary lipid combinations at systemically varied ratios we highlight liposomal formulations of intermediate stability, what we termed „the edge of stability", requiring moderate stimuli for destabilization. Supplementation with a pH-sensitive cholesterol derivative (to obtain acid labile liposomes) and renewed assessment with cargo load led to the discovery of three formulations with sufficient shelf-life stability, acceptable cargo retention and efficient pH-responsive cargo release *in vitro*. The "lead candidates" exhibited promising *in cellulo* uptake with increased intracellular cargo release and revealed *in vivo* performance advantages compared to a control liposome. Our approach filters lipid compositions on "the edge of stability" that were introduced with a pH-sensitive cholesterol derivate leading pH-responsive liposomes, out of a multidimensional parameter space. Their discovery by rational approaches would have been highly unlikely, thus highlighting the potential of our screening approach.

1. Introduction

The stability of its lipid bilayer membrane is a defining characteristic of a liposome, which governs the retention, transport, and eventual release of an encapsulated cargo in fields ranging from fundamental research[1] over cosmetics[2] to medical applications.[3] Since the first liposomal medical treatment was approved in 1995,[4] a vast amount of data, clinical and other, became available, which focused on increasing liposome stability to overcome fast clearance within the body[5] and to decrease side effects.[6] Major issues being addressed by current research include drug delivery by active or passive targeting,[7] liposome penetration of target tissues,[8] incorporation of cationic lipids for DNA and RNA delivery[9] and efficient release of small molecule cargo.[10] This latter aspect in particular is crucially related to stability, and the object of our research.

Many molecular and biophysical concepts and corresponding compounds were put forward to address the partially contradictive requirements for liposomal stability versus release at a therapeutically relevant site.[11] Among various factors that may contribute to stability and release, the biophysical stability

[a] *L. Gleue,[+] M. Voigt,[+] M. Helm*
Institute of Pharmaceutical and Biomedical Sciences, Johannes Gutenberg University, Staudingerweg 5, 55128 Mainz, Germany
E-mail: mhelm@uni-mainz.de

[b] *B. Graefen,[+] J. Schupp,[+] M. Fichter, M. Kuske, V. Mailaender, A. Tuettenberg*
Department of Dermatology, University Medical Center of the Johannes Gutenberg University Mainz, Langenbeckstr. 1, 55131 Mainz, Germany
E-mail: antuette@uni-mainz.de

[c] *D. Schneider*
Department of Chemistry-Biochemistry, Johannes Gutenberg University, Hanns-Dieter-Hüsch-Weg 17, 55128 Mainz, Germany

[d] *M. Fichter, V. Mailaender*
Max Planck Institute for Polymer Research, Ackermannweg 10, 55128 Mainz, Germany

[e] *M. Fichter, M. Kuske, V. Mailaender*
Paul-Klein-Center for Immunintervention, University Medical Center of the Johannes Gutenberg University Mainz, Langenbeckstr. 1, 55131 Mainz, Germany

[f] *A. Tuettenberg*
Research Center for Immunotherapy, University Medical Center of the Johannes Gutenberg University Mainz, Langenbeckstr. 1, 55131 Mainz, Germany

[g] *M. Voigt[+]*
BioNTech SE, An der Goldgrube 12, 55131 Mainz, Germany

[h] *J. Schupp[+]*
Frankfurt Cancer Institute, Paul-Ehrlich-Straße 42–44, 60596 Frankfurt, Germany

[i] *J. Schupp[+]*
Goethe University Frankfurt, Institute of Neurology (Edinger Institute), Heinrich-Hoffmann-Straße 7, 60528 Frankfurt, Germany

[j] *M. Kuske*
Institute for translational oncology Mainz (TRON-Mainz), Freiligrathstraße 12, 55131 Mainz, Germany

[+] *authors contributed equally*

Supporting information for this article is available on the WWW under https://doi.org/10.1002/cmdc.202400648

of the liposomal membrane is an attractive target for rational manipulation, because the membrane lipid order can be described by basic thermodynamic concepts. Below the phase transition temperature (T_m), lipids are in the gel phase, whereas above the T_m, they are in the liquid crystalline phase.[12] Membranes in lipid crystalline phase are more fluid than membranes in gel phase, which are more permeable to small molecules, and are therefore less effective in retaining encapsulated cargo.[13] The T_m of a pure lipid is specific, and depends on its fatty acid chain length, saturation and head group. In contrast, it can be roughly estimated, but not accurately predicted for binary lipid mixtures, even when the T_m values of the components are known.[14,15] However, liposomal stability can still be rationally manipulated by certain destabilizing lipids, which do not form lamellar phases on their own. Their addition decreases stability and T_m of lipid membranes. Liposomal membranes can also benefit from a "molecular plug" effect caused by incorporation of cholesterol into the liposomal membrane, which can decrease membrane permeability while increasing its stability.[16] More recent efforts focused on liposomal formulations, which change membrane permeability in response to therapeutically relevant stimuli such as heat,[17] or pH.[10e,18,20]

For our study concept "Liposomal formulations on the edge of stability", we hypothesized that a stimulus-dependent cargo release requires a liposomal formulation of minimum stability, and that a stimulus must then supply the energy needed to rupture the liposomal membrane. Liposomes would require that minimum stability to retain their cargo until arrival at a therapeutic location, but overly stable liposomes would fail to open upon a stimulus such as heat or pH change. This brings a need for tuning liposomal stability to that delicate balance, which we have taken to call "the edge of stability".

Many liposomal formulations for classical non-stimulus responsive liposomes share common components, e.g. fully saturated lecithins in combination with cholesterol, while DPPC features in thermo-sensitive liposomes.[17] A combination of DOPE and DOPC with cholesterylhemisuccinate (CHEMS) leverages its pK_a of ~pH 5.5 as a molecular concept for acid-triggered cargo release from liposomes.[10e,,18b,19–21]

A relatively high variety of modifying lipids, often of experimental/exploratory nature, were reported in liposomal formulations, reflecting the need for improved performance and the potential of a vast 'lipid-composition-space', most of which are essentially unexplored.[22] Therefore, we implemented a combinatorial and largely unbiased approach. We postulated that in liposomes whose membranes are composed of two lipids, membrane stability can be tuned through the lipid ratio. Upon addition of increasing amounts of a destabilizing lipid to a lipid that can sustain liposome formation by itself, increasingly unstable liposomes would form up to the edge of stability, beyond which no more liposome formation is observed. For a given binary lipid combination the goal would then be to determine the amount of destabilizing lipid that would still allow the postulated minimum stability. In the perspective of a molecular concept, the resulting liposomes were to be further developed by addition of CHEMS[10e,19a] to confer a pH-sensitive molecular entity.

We needed an experimental approach to determine or approximate liposomal stability, and a medium-to-high throughput formulation technique to produce liposomal formulations for screening in large numbers in small amounts. The latter prerequisite is met by the dual centrifugation technique (DC). DC, an 'in vial' homogenization technique, allows fast preparation of up to 40 individual liposome samples in parallel, controllable diameters and variation in batch sizes, starting with single digit milligram amounts.[,23a,24,25] Caveats include polydispersion index (PI) values that are relatively high in comparison to other techniques such as extrusion, thereby limiting perspectives for advanced development of studies *in vivo*. With these limitations in mind, the present work does not directly aim at the development of a ready-to-use formulation of a defined payload drug in a fully defined liposome. Rather, our intention is to demonstrate a screening approach by DC with different payloads, that can identify promising lead candidates. Arguably, a full development of such leads with a defined payload will require reevaluation, and may need a switch in later stages to more controllable process such as extrusion.[25,26]

Materials and Methods

Consumables, Devices and Cells

Chemicals and Consumables

DMPC (#850345C-200mg), DODAP (#890850C-25mg), DOPC (#850375C-200mg), DOPE (#850725C-200mg), DOPG (#840475C-200mg), DOTAP (#890890C-200mg), DPPC (#850355C-200mg), DPPG (#840455P-200mg) and Laurdan (#850582P) were obtained from Avanti Polar (Alabaster, Alabama, USA). Biocoll® (#L6115) (Bio&Sell GmbH, Feucht, Germany); Chloroform (#37331.2), Ethanol (#5054.3), Methanol (#KK39.2), Paraformaldehyde (#0964.2) and Triton-X100 (#3051.3) were received from Carl Roth GmbH & Co. KG (Karlsruhe, Germany). 100 mm culture petri dishes (#430167), 24 well plates (#3527), 96 well plates (#3598) and round bottom polystyrene test tubes (#352008) were obtained from Corning Inc. (Corning, Ney York, USA). Sephacryl S500-HR slurry (#GE17-061301) was used purchased from GE Healthcare (Chicago, USA). 50 ml tubes (#227261) and 96-well optical bottom plate black (#10706172) were obtained from Greiner Bio-One GmbH (Frickenhausen, Germany). Ampuwa® (#B230673) was ordered from Fresenius Kabi (Bad Homburg, Germany). 8 well μ-slides (#80826) was obtained from Ibidi GmbH (Gräfelfing, Germany). Recombinant human M–CSF (#11343117) was purchased from ImmunoTools GmbH (Friesoythe, Germany). Primocin® (#ant-pm-2) was obtained from InvivoGen (San Diego, California, USA). PCR tubes 200 μL (#G001-F) was received from Kisker Biotech GmbH & CO. KG (Steinfurth, Germany). Calcein (#C0875-5G), Cholesterol (#C8667-25G), Doxorubicin hydrochloride (#D1515-10MG), Potassium chloride (#P9541-500G), Resazurin sodium salt (#7017), RPMI1640 (#R7509), Sulforhodamine B (#230162-5) and Water (ultra pure) (#ZRQSVR5WW) were obtained from Merck KGaA (Darmstadt, Germany). HPLC vials (#EC-1026 + #7-0632 + #7-0693) were obtained from neoLab Migge GmbH (Heidelberg, Germany). Heparin-sodium (#PZN: 16200037) was purchased from PANPHARMA GmbH (Trittau, Germany). Isoflurane (PZN: 09714675) was purchased from Piramal Critical Care (Voorschoten, Netherlands). NeuroDiD (#PK-

CA707-60014) and Hoechst 33258 (#PK-CA707-40046) were obtained from PromoCell GmbH (Heidelberg, Germany). 1.5 ml reaction tubes (#72.706) were purchased from (Sarstedt AG & CO. KG, Nümbrecht, Germany). SiLiBeads® Typ ZY-S 0.3–0.4 mm (#96035-362) was received from Sigmund Lindner GmbH (Warmensteinach, Germany). Accutase® (#00-4555-56), DiD (#D7757), DiR (#D12731), Fetal calf serum (#10500-064), GlutaMAX™ (#35050038), Human serum (#31876), Phosphate buffered saline (#14190094), Trypsin-EDTA (0.05 %) (#25300054) and Viability Dye eFluor™ 780 (#65-0865-18) were ordered by Thermo Fisher Scientific (Waltham, Massachusetts, USA).

Liposome Formulation by Dual Centrifugation

The lipids used for liposome preparation are shown in Table 1. Liposomes were prepared *via* dual centrifugation with a modified protocol as previously described.[23b,24a] Lipids were dissolved in absolute ethanol, chloroform or chloroform:methanol:water (2:1:0.1) in stock concentrations of 20 mg/mL and combined in PCR tubes to yield 2 and 5 μmol of the intended compositions for the laurdan fluorescence and all other experiments, respectively. 1 mg/mL laurdan in methanol and membrane dye DiD or DiR in ethanol were added for laurdan and cell experiments to yield 0.1 mol-% of the total lipid amount, respectively. Combined lipids were pre-dried in a SpeedVac® (Eppendorf SE, Hamburg, Germany) vacuum centrifuge at 30 °C overnight and then lyophilized with Alpha 2–4 LD (Christ Gefriertrocknungsanlagen GmbH, Osterode im Harz, Germany) for at least 48 h to completely remove solvents. The integrity of the lipid compounds was tested by thin-layer chromatography (Figures S1 and S2, Section Sup. 2). Thoroughly dried lipid compositions were kept at −20 °C until usage. For preparation of a vesicular phospholipid gel, following volumes were used and scaled linearly with the lipid amount. 5 mmol dried lipids were incubated for 10 minutes with 9.3 μL of cargo solution. As cargo, 50 mM sulforhodamine B (SRb), 20 mM calcein (CAL) or 50 mg/mL doxorubicin hydrochloride (DXR) in water were used. After addition of 350 mg of 0.3–0.4 mm ceramic SiLiBeads®ZY, samples were subjected to dual centrifugation in Zentrimix 380R (Hettich GmbH, Tuttlingen Germany), at 2500 RPM and 25 °C for 20 min. The resulting vesicular phospholipid gel was diluted with 77.2 μL phosphate buffered saline (PBS) and subjected to dual centrifugation again at 2500 RPM and 25 °C for 2×2 min while turning the sample tray between the runs to form liposomes.

Evaluation of Liposome Stability Using Laurdan Fluorescence Spectroscopy

10 μL of liposome stock solutions with PBS as cargo were diluted 5x in PBS and subjected to a black 96-well polypropylene optical bottom plate. Fluorescence measurements were performed in a M200 Pro multiplate reader (Tecan, Männedorf, Switzerland) at 388/440 nm (Ex./Em.) and 388/490 nm (Ex./Em.) to determine the fluorescence emission intensities at 440 nm (I_{440}) and 490 nm (I_{490}), respectively. The laurdan generalized polarization value (LGP)[12] was calculated using Equation (1).

$$LGP = \frac{(I_{440} - I_{490})}{(I_{440} + I_{490})} \quad (1)$$

The obtained LGP-values were normalized to simplify the resulting graphs. The LGP value of liposomes with 100 mol-% lipid 1 (Table 2) was set to 0 % deviation and the LGP value of the respective liposomes with 10 mol-% lipid 1 and 90 mol-% lipid 2 was set to 100 % deviation. The % of deviation from lipid 1 (%dev) was plotted against increasing mol-% of lipid 2 and fitted with a sigmoidal, 4PL, X is concentration fit with least squares as fitting method (see Equation (2)) using GraphPad Prism 9 (GraphPad Software, Boston, Massachusetts, USA).

$$y = \text{bottom value} + \frac{(\text{top value} - \text{bottom value})}{(1 + 10^{((\log EC50 - x) * \text{HillSlope})})} \quad (2)$$

Determination of Encapsulation Efficiency, Cargo Release and Retention by Size-exclusion Chromatography

To remove non-encapsulated cargo, liposome stock solutions were subjected to 1.5 mL glass vials for automated size-exclusion chromatography by HPLC (1100 Series, Agilent Technologies, Santa Clara, California, USA). The body of an UNO Q1 column (Bio-Rad, Hercules, California, USA), cleared and self-packed with 2 mL Sephacryl S500-HR slurry was used as chromatography column. Purification resulted in 600 μL of purified liposomes and a free cargo fraction. Encapsulation efficiencies (EE) were calculated by dividing absorption intensity of the used cargo (calcein & doxorubicin at 490 nm, sulforhodamine b at 550 nm) within the purified liposome fraction (L) by the total absorption intensity multiplied by 100 % (Equation (3)).

Table 1. Abbreviation list for used lipids and membrane supplements.

Abbreviation	Full name	Abbreviation	Full name
CHEMS	cholesterylhemisuccinate	DOPC	1,2-dioleoyl-*sn*-glycero-3-phosphocholine
CHOL	cholesterol	DOPE	1,2-dioleoyl-*sn*-glycero-3-phospho-ethanolamine
EPC	egg phosphatidyl choline	DOPG	1,2-dioleoyl-*sn*-glycero-3-phospho-rac-(1-glycerol) sodium salt
DiD	1,1′-dioctadecyl-3,3,3′,3′-tetramethylindodicarbocyanine 4-chlorobenzenesulfonate salt	DOTAP	N-[1-(2,3-dioleoyloxy)propyl]-N,N,N-trimethylammonium chloride
DiR	1,1′-dioctadecyl-3,3,3′,3′-tetramethylindotricarbocyanine-iodide	DPPC	1,2-dipalmitoyl-*sn*-glycero-3-phosphocholine
DMPC	1,2-dimyristoyl-*sn*-glycero-3-phosphocholine	DPPG	1,2-dipalmitoyl-*sn*-glycero-3-phospho-rac-(1-glycerol) sodium salt
DODAP	1,2-dioleoyl-3-dimethylammonium-propane	laurdan	1,1′-dioctadecyl-3,3,3′,3′-tetramethylindodicarbocyanine

Table 2. Lipids and lipid combinations (L) used for liposome screening. **A** Binary lipid composition mixtures. Information of a sigmoidal progression of lipid mixture (laurdan assay, see Figure 2) is listed by check symbol. Candidates identified in Section 2.3.2., are highlighted in color (L2, L11, L15). **B** and **C**: Lipid properties are displayed as lipid netto charges at pH 7.4 (pH 5.5), fatty-acid chain lengths (carbon atoms:double bonds) and phase transition temperatures T_ms for stabilizing lipids in **B** and modifying lipids in **C**. For abbreviations of lipids, see methods section Table 1.

A

Lipid combination (L)	Stabilizing lipid 1	Modifying lipid 2	Sigmoidal LGP?
L1	DMPC	DOPE	
L2		DODAP	✔
L3		DOTAP	
L4	DPPC	DOPE	✔
L5		DODAP	
L6		DOTAP	✔
L7	DPPG	DOPE	
L8		DODAP	
L9		DOTAP	✔
L10	DOPC	DOPE	
L11		DODAP	✔
L12		DOTAP	
L13	DOPG	DOPE	
L14		DODAP	✔
L15		DOTAP	✔
L16	EPC	DOPE	
L17		DODAP	
L18		DOTAP	

B

Stabilizing lipid 1	Chain lengths[1]	T_m (°C)[1]	Lipid charges[1]
DMPC	14:0	24	0
DPPC	16:0	41	0
DPPG	16:0	41	-1
DOPC	18:1	-17	0
DOPG	18:1	-18	-1
EPC	variable	variable	0

C

Modifying lipid 2	Chain lengths[1]	T_m (°C)[1]	Lipid charges[1]
DOPE	18:1	-16	0
DODAP	18:1	-	0 (+1)
DOTAP	18:1	0	+1

[a] Values obtained from.[31]

$$\%EE = \frac{\text{absorption L}}{\text{total absorption}} \times 100\,\% \quad (3)$$

For determination of cargo release, 100 μL of SEC purified liposomes were incubated at pH 5.5 and 37 °C for 4 h to simulate lysosomal conditions and subjected to SEC for purification again. To determine long-term cargo leakage, purified liposomes were kept at pH 7.4 and 5 °C for 1 week and purified again. Cargo release was calculated by dividing the absorption intensity of the respective cargo within the free cargo fraction (FC) by the total absorption intensity multiplied by 100% (Equation (4)). Cargo retention was therefore calculated as 100% minus %release.

$$\%release = \frac{\text{absorption FC}}{\text{total absorption}} \times 100\,\% \quad (4)$$

For serum stability experiments, liposomes were incubated for 4 h at 37 °C in full human serum.

Liposome Loading Analysis

Doxorubicin-loaded liposomes and unloaded liposomes were each mixed with 5% (v/v) Triton-X100 dissolved in PBS. Doxorubicin absorbance of triplicates was measured at 488 nm using a Sense Beta Plus Microplate Reader in 96 well plates (total volume 200 μl/well). Unloaded liposome sample values were subtracted from corresponding doxorubicin loaded liposomes. Loading efficacy was then calculated by applying linear regression to a 1:2 dilution series of doxorubicin from 108 μM to 0.1 μM in Microsoft Excel. Total volume needed for treatment with 1 μM doxorubicin-loaded liposomes was then further calculated for cell treatment assays.

Physicochemical Characterization by Dynamic Light Scattering (DLS)

Size, polydispersity (PDI) and zeta potential (ζ-potential) of 20 μL purified liposome sample were determined using a Malvern Zetasizer Nano Series (Malvern Panalytical, Malvern, United Kingdom) in a folded disposable capillary cell at 25 °C after an equilibration time of 30 s. Liposome samples were diluted in 1 mL of freshly filtered aqueous 10 mM potassium chloride solution for zeta potential analysis or in phosphate-buffered saline for size and size distribution. Each sample was measured in triplicate in 30 runs. The viscosity of the water was set to 0.8872 cP, with a refractive index of 1.33, a scattering angle of 173° and an automatic selection for the attenuation index and voltage.

Human Macrophage Culture

Human peripheral blood mononuclear cells (PBMC) were isolated from buffy coats obtained from healthy volunteers, with approval by the local ethical committee (Landesaerztekammer Rhineland-Palatinate No. 837.019.10 (7028)) *via* Biocoll density gradient centrifugation. 200 million PBMC were seeded in RPMI1640, supplemented with 1% Glutamax™, 0.2% Primocin®, and 50 ng/mL M–CSF in cell culture petri dishes for 1 h in a 37 °C 5% CO_2 incubator. After 1–2 h non-adherent cells were rinsed off by repeated washing of the petri dishes with pre-warmed to 37 °C PBS checked by microscopy. Adherent cells (monocytes) were cultured in the medium described above containing an additional 1% heat

inactivated human plasma for six days. Macrophages were harvested using Accutase™.

Human Plasma

Human plasma of ten healthy donors was pooled in 2×50 ml tubes and centrifuged for 15 min at 800× g. The supernatant was pooled and centrifuged for 15 min at 1000× g to deplete the cellular contents. The collected supernatant (plasma) was then heat inactivated for 20 min at 56 °C. Insoluble denatured protein was removed by centrifugation at 3000× g for 15 min at room temperature. Heat inactivated plasma was stored at −20 °C until further use.

Melanoma Cell Line UKRV-Mel-15 a

Human melanoma cells from cell line UKRV-Mel-15a (obtained from Dr. A. Paschen in 2014 (Essen, Germany)) were cultured in RPMI-1640 medium supplemented with 10% fetal calf serum, GlutaMAX™ and Primocin®. After reaching approximately 80% confluence, cells were harvested with Trypsin-EDTA solution and reseeded in a higher dilution. This cell line has been validated *via* short tandem repeat (STR) analysis (Eurofins Genomics) last in 08/2022. The resulting STR profiles matched with the online databases of the German collection of microorganisms and cell cultures (DSMZ) (Available online: https://www.dsmz.de/services/human-and-animal-cell-lines/online-str-analysis).

Flow Cytometry

Human macrophages were seeded in 24 well plates at a density of $2{,}5*10^5$ cells per well in 1 mL of culture medium. Human melanoma cells (UKRV-Mel-15a) were seeded in 24 well plates at a density of $5*10^4$ cells per well in 1 mL of culture medium. Cells were treated in triplicates with 1 μM doxorubicin loaded within liposomes (volumes were estimated by doxorubicin loading analysis), 1 μM free doxorubicin or left untreated as control. After 30 minutes and 4 h treatment cells were harvested by using trypsin-EDTA (melanoma) or Accutase™ (macrophages). Dead cells exclusion was achieved by using Fixable Viability Dye eFluor™ 780. Afterwards, cells were fixed by using 4% paraformaldehyde dissolved in PBS for 30 min. Flow cytometry analysis was performed on an LSRII cytometer (BD Biosciences, Heidelberg, Germany). Data were analyzed using Cytobank (Beckman Coulter, Brea, California, USA).[27]

Cell Viability Assay (Resazurin)

Human macrophages were seeded in 96 well plates at a density of $5*10^4$ cells per well in 0.2 mL of culture medium. Human melanoma cells (UKRV-Mel-15a) were seeded in 96 well plates at a density of $1*10^4$ cells per well in 0.2 mL of culture medium. Cells were treated in triplicates with either liposomes loaded with 1 μM of doxorubicin (volumes were estimated by doxorubicin loading analysis) or equivalent volumes of unloaded liposomes, 1 μM free doxorubicin or left untreated as control. After 24 h and 72 h treatment, medium was replaced with resazurin sodium salt dissolved in PBS at a final concentration of 6 μg/mL. Cells were incubated for 1 h at 37 °C. Fluorescence was measured at 544/590 nm (excitation/emission) using a Sense Beta Plus Microplate Reader (Hidex Oy, Turku, Finland). Fluorescence values were blank corrected and normalized to untreated sample in Excel (Microsoft Corporation, Redmond, Washington, USA), graphs were created in GraphPad Prism 9.

Intracellular Doxorubicin Release/Staining (Microscopy)

Human macrophages were seeded in 8 well μ-slides at a density of $7.5*10^4$ cells per well in 0.3 mL of culture medium. Human melanoma cells (UKRV-Mel-15a) were seeded in 8 well μ-slides at a density of $1.5*10^4$ cells per well in 0.3 mL of culture medium. After 30 minutes and 4 h treatment with 1 μM of loaded doxorubicin (volumina were estimated by doxorubicin loading analysis), 1 μM free doxorubicin or left untreated, the cells were fixed by using 4% paraformaldehyde dissolved in PBS for 30 min. Hoechst 33258 in PBS at 10 μM was used to stain the nuclei. Cell membranes were stained using the green-fluorescent cytoplasmic membrane staining kit on fixed cells. Images were acquired with a Leica TCS SP8 (Leica Microsystems, Wetzlar, Germany) and analyzed using the Fiji ImageJ (National Institutes of Health, Bethesda, Maryland, USA) distribution.[28]

Ethical Approval Statement (Mice Experiments)

The biodistribution study of liposomal lead candidates without cargo in mice was carefully evaluated and approved by local authorities (G20-1-123, Landesuntersuchungsamt Rhineland-Palatinate, Germany). *In vivo* biodistribution study was necessary for the evaluation of elimination from blood stream and distribution of the liposomal candidates in a complex organism. A total of 26 female mice of B6 N-Tyrc-Brd/BrdCrCrl („B6 Albino") (Strain code 493) with an average age of $\geq$7 weeks and body weight between 17–20 g were used with each mouse as an experimental unit. Sample size and group size was based on prior experimental studies, without exclusion criteria.[29] The mice were purchased from Charles River. The mouse were housed under a 12 h dark-light cycle at a constant temperature and with ad libitum feeding on water and standard laboratory mice chow. The experiment was performed after one week of adaptation in the Paul-Klein-Zentrum für Immunintervention (Building 308 A) of the University medical center of the Johannes Gutenberg-University in Mainz after random assignment. Potential confounders were not controlled and the experimenters were aware of the group allocation by housing each treatment group in an own cage. Experiments were performed in accordance with relevant laws and institutional guidelines. Differences between groups with a significance level of $p \leq 0.05$ (student's t-test) were considered statistically significant.

In vivo biodistribution

Background fluorescent signal images of animals were acquired under 2.5% isoflurane oxygen anesthesia in the IVIS Spectrum CT (Perkin Elmer, Waltham, Massachusetts, USA) for 2 seconds exposure time with 745/800 nm (Ex/Em). 5 ml/kg bodyweight lipid-nanocarrier labeled with 0.2 mol-% fluorescence DiR (L0, L2C, L11C, L15C) were then injected intravenously (i.v.) in the tail vein ($n=5$ for each nanocarrier). The control groups received PBS or DiR dissolved in PBS, respectively (DiR was dissolved in 1% ethanol) ($n=3$ for each control). After injection, mice fluorescence intensities were imaged first time under 2.5% isoflurane anesthesia at time point "0 h". 3 h and 24 h after injection 2–3 drops of blood were collected in 1.5 ml tubes (with 2 μl heparin-sodium) from the mice before imaged, while anesthetized with 2.5% isoflurane oxygen. After the final measurement at 24 h mice were euthanized by cervical dislocation. DiR control was used as an additional control to PBS and measured data for DiR were not significantly varying from PBS control, resulting in the exclusion of the data from all following analyses.

Ex vivo Organ Analysis

The abdomen was opened in one mouse from each group and imaged in the IVIS CT. Fluorescent organs (liver, spleen) were collected in 6 well plates with 2 ml PBS in each well. Organs from each group were then dried, placed on a black plate and imaged with IVIS CT for 0.5 seconds exposure time.

Image Analysis

In vivo images were analyzed using Living Image version 4.5.2. software (Perkin Elmer, Waltham, Massachusetts, USA). For *in vivo* imaging, the abdomen area was defined as area between the sternum and middle of the abdominal area. Region of interest (ROI) was drawn in the defined area with ROI size copied for each picture and kept for all *in vivo* images. The min and max values of epi fluorescence were adjusted to the same min and max values for each *in vivo* image to make them visually comparable (Min: 3.50×10^8, Max: 1.50×10^9 Radiant Efficacy). ROIs were quantified in the physical, calibrated unit "Total Radiant Efficiency [p/s]/[μW/cm^2]". Tissue autofluorescence of the mice was subtracted from the ROI values measured after injection of the labeled lipid-nano-carriers. Total sample number of animals was 26. *Ex vivo* images were analyzed similarly. After adjusting the min and max values for each *ex vivo* image the ROI size was kept for all livers and a separate ROI was kept for all *ex vivo* images for the spleen. Total sample number per organ was 26.

Blood Fluorescence Analysis

Blood samples were taken 3 h and 24 h after sample injection from vena facialis. For fluorescent analysis, 25 μL blood were diluted in 175 μl PBS and fluorescence was measured in a 96-well flat bottom black well with Spark 10 M multiplate reader at 740/780 nm (Ex./Em.). Total sample number for blood samples was 2×26. Fluorescence was measured for each sample in triplicates. Blank corrected values from each time point were normalized to average PBS value. Subsequently 24 h values of treatment groups were normalized to 3 h values of each treatment group.

2. Results & Discussion

2.1. Study Design, Caveats and Limitations

This study followed a workflow (Figure 1) for a physicochemistry-based screening of large sample numbers of liposomal formulations. The latter contained systematically variegated lipid compositions to reveal lipid compositions where membrane stability transitions into membrane instability ("at the edge of stability"). We deliberately omitted cholesterol and its derivatives in Section 2.2., because the equalizing effect of such "molecular plug" compounds on membrane stability were anticipated to impair the detection of membrane transitions at "the edge of stability". Subsequent embedment of CHEMS implemented pH-stimulated release of encapsulated cargo by acidic while sustaining maximum retention upon storage (described in Section 2.3.). Lead formulations identified in Section 2.3. were tested *in cellulo* (described in Section 2.4.) and *in vivo* (described in Section 2.5.).

2.2. Evaluation of Membrane Stability (Stage 1)

Two lipid panels were categorized into "stabilizing" and "modifying" lipids according to literature, ignoring aspects of suitability in clinical studies, known biological effects, and toxicity. Permutations of these two lipid panels lead to 18 "simplified" lipid compositions, i.e. binary lipid mixtures (numbered L1 through L18) (Table 2A). Some of the liposome-forming "stabilizing" lipids in Table 2B and C were chosen such as to represent different properties like charge, T_m and fatty acid chain length. The "modifying" lipids shown in Table 2C have identical fatty acid chain lengths and T_ms below preparation temperature (25 °C), hence an impact on membrane stability was supposed to derive mainly from their charge and miscibility with lipid 1.

Lipid compositions were prepared using dual centrifugation, with ratios varied in 10 mol-% steps, starting from 100 mol-% of stabilizing lipid 1, with stepwise substitution of modifying lipid 2 up to 90 mol-%. Given that the 100 mol-% lipid 1 samples

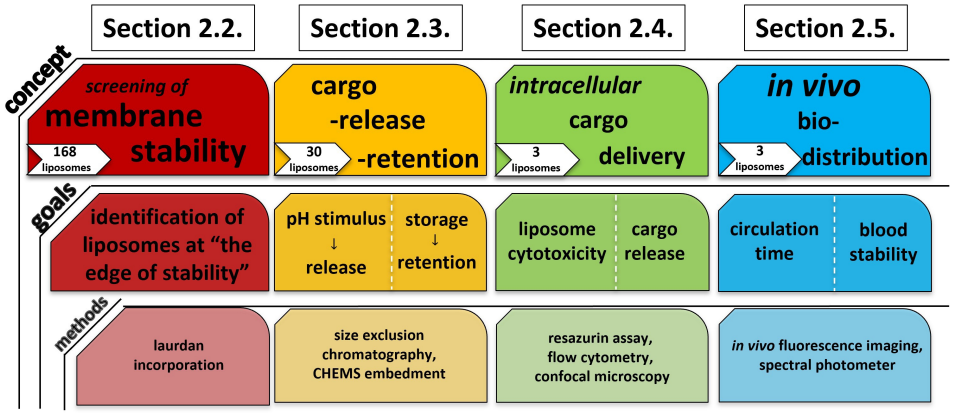

Figure 1. Visual concept of screening workflow with goals and methods. The manuscript sections corresponding to the performed steps are indicated.

were identical in all three series of lipid 2 permutations, the total number amounted to 168 different lipid compositions. To monitor lipid phase transitions upon increasing content of destabilizing lipids, we incorporated 0.1 mol-% of the hydrophobic fluorescent dye laurdan into liposomal membranes during preparation, expecting a characteristic sigmoidal curve. The fluorescent properties of laurdan depend on the polarity of its intimate environment and any changes (e.g. in lipid packing) result in an altered fluorescence emission at two wavelengths. This means properties are significantly affected upon membrane destabilization, e.g. when polarity of the environment increases due to surrounding water molecules.[30] Changes in the laurdan fluorescence emission are given as laurdan generalized polarization (LGP) value.[12b,15]

Within a ratio series we observed either constant increase or constant decrease of the LPG value (Figure S3). The properties of lipid 1 might explain some of the values. For example, in liposomes containing DPPC (L4–L6) or DPPG (L7–L9) as main stabilizing lipid with T_m above ambient temperature (25 °C), the lipids are in rigid gel phase and the LGP decreases upon membrane destabilization.[12b] For the other class-1-lipids (Table 2B), the T_m is lower than 25 °C and these lipids are therefore in the liquid-crystalline phase. As the only type 1 lipid, none of the lipid combinations including EPC led to a sigmoidal curvature in any combination, possibly due to the heterogeneity of the EPC lipid composition.[12]

After excluding lipid combinations without a sigmoidal shape or with low changes in the overall LGP values we had 7 promising lipid compositions left (namely L2, L4, L6, L9, L11, L14 and L15) for which normalized LGP values are plotted against increasing mol-% of lipid 2 in Figure 2. Liposomes containing 100 mol-% lipid 1 (0 mol-% of lipid 2) were normalized to 0% deviation, and liposomes containing 90 mol-% of lipid 2 corresponded to 100% deviation. Note that, for better visualization, the absolute (rather than the relative) deviation is shown.

Interestingly, the data in Figure 2 suggested that the composition range of 20–40% of lipid 2 is frequently encountered at "the edge of stability", as highlighted in Figure 2 in grey. For the subsequent studies, we focused on these as potential candidates for further development.

2.3. Determination of Cargo Release and Retention Behavior (Stage 2)

To assess shelf-life, we established a protocol for measuring retention and release, using hydrophilic dyes as model cargos. Data presented below pertain to sulforhodamine b (SRb) as model cargo, but key data were recapitulated with other dyes also representing model cargos for small hydrophilic molecules (vide infra). SRb was the cargo of choice, because its absorption at 550 nm is independent of pH value in buffered medium, which prevents biases when comparing data from pH 7.4 with pH 5.5.[32] SRb was encapsulated by DC, and non-encapsulated cargo was subsequently removed *via* size exclusion chromatography (SEC). Figure 3 shows an SEC elution profile measured by UV absorption of SRb at 550 nm, revealing two populations, namely encapsulated SRb eluting with the liposomes (L) at ~1 min and free cargo (FC) SRb eluting at ~2–5 min.

Encapsulation efficiencies (EE) were calculated as the ratio of SRb absorption signal in the liposome fraction L relative to that of L plus free cargo fraction, consistently showing EEs of 30–50% (Figure S4). Data are consistent with the vast majority of the cargo being encapsulated, although we cannot exclude that minor amounts might adhere to the liposomal surface.

Furthermore, as an *in vitro* mimic of acidic lysosomal conditions after liposome endocytosis, an aliquot of the purified liposomes was incubated at pH 5.5 and 37 °C for 4 h.[33] Thereafter, liposomes were submitted to SEC again and the cargo release was determined as the ratio of SRb absorption signal in FC relative to that of L + FC (see Equation (4) in the methods section). The remainders of the purified liposomes were stored

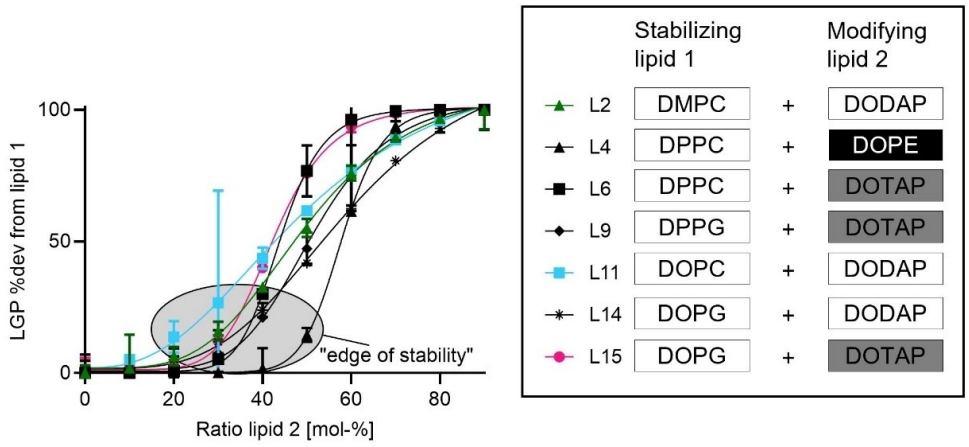

Figure 2. Laurdan assay curve progression Laurdan assays of lipid mixtures L2, L4, L6, L9, L11, L14, L15 (n = 3). LGP values as deviation percentage from lipid 1 were plotted against increasing mol-% of modifying (destabilizing) lipid 2 as described in Materials and Methods. Liposomes within the grey circle of the graph were identified as potentially "at the edge of stability" formulations. Lipid compositions are displayed right side of the figure in black box. Lead candidates found in Section 2.3.2. are highlighted in color.

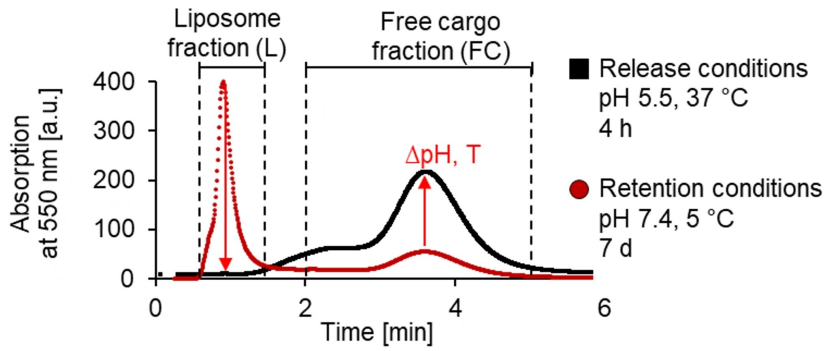

Figure 3. Determination of liposome cargo release and retention by SEC. A typical chromatogram obtained after separation of free cargo from intact liposomes by SEC is shown. Cargo encapsulation efficiency, release after 4 h incubation at pH 5.5 and 37 °C and retention after incubation for 1 week at pH 7.4 and 5 °C were calculated as described in the methods section. Model cargos sulforhodamine b and calcein were quantified by absorption at 550 and 490 nm, respectively.

at 5 °C for 1 week and then again analyzed to determine cargo retention under normal shelf conditions.

2.3.1. Mapping "The Edge of Stability" in Selected Binary Composition Liposomes

From the lipid combinations L2, L4, L6, L9, L11, L14 and L15 identified above, initial characterizations compared performances of liposomes containing 20, 30, and 40 mol-% type-2 lipid and additionally 0 and 10 mol-% for L6 and L9 and for L4 from 0–70 mol % (Figure 4A).

Overall the optimal performance was observed at 30 mol-% for the 4 lipid combinations L2, L11, L14 and L15. While a content of modifying lipid 2 below the edge (e.g. 20 mol-%) led to more stable liposomes with high cargo retention, it simultaneously caused lower release (exception L2). Inversely, higher amounts of lipid 2 (e.g. 40 %) resulted in insufficient stability and retention (see Figure 4A). We set 80 % as the minimum release as an arbitrary parameter for selection of formulations, which was reached by L11, L14 and L15 at 40 mol-% of lipid 2.

L6, and L9 presented interesting cases, which did not reach the self-set limitation, since 30 and 40 mol-% type 2 lipid in L6 did not come with an acceptable retention, while L9 came with low release capability. Here we extended the range to 0 mol-% type 2 lipid resulting in high release with higher retention for 10 mol-% of lipid 2, but still leading to exclusion for L9 with release of only 72 %. For L4 we applied a similar approach, but were unsuccessful even though increasing type 2 lipid from 0 to 70 mol-% substitution leading to exclusion.

Physicochemical characterization of respective lipid combinations *via* dynamic light scattering (DLS) indicated the start of liposome destabilization by an increase of sizes except for L9, PDIs (Figure 4B) and a drop in encapsulation efficiency (Figure S5), plausibly going along with the low cargo retention. Additionally, candidate L9 did not show a steady increase of retention with a stepwise increase of lipid 2 in 10 mol % increments.

Including the narrated "excursions" in the L4, L6 and L9 series brought the liposomal formulations under "advanced scrutiny" to a total of 30 (Figure 4A). Of these 30, 5 formulations showed retention and reached a release of 80 %. These formulations, marked with a grey rectangle in Figure 4A, were termed L2e, L6e, L11e, L14e and L15e as identified as "the edge of stability" formulations. Figure 4A clearly shows that the retention characteristics needed further improvement.

2.3.2. Addition of CHEMS as a pH-sensitive "Molecular Plug"

Since most successful developments contain at least three lipids, typically including a cholesterol-derivative, we introduced cholesterylhemisuccinate as a third compound. We started with low concentrations of 5 and 10 mol-%, which were added to the liposome mixtures L2e, L6e, L11e, L14e and L15e. The resulting liposomes, termed L2c, L6c, L11c, L14c and L15c, were tested for cargo release and retention at pH 5.5 and 37 °C. Additionally, we measured retention after 4 h incubation at physiological pH and 37 °C to differentiate between temperature and pH triggered release.

Figure 5A shows the results of the 5 leading candidates containing 5 or 10 mol-% CHEMS (with composition listed in Figure 5B), compared to a conventional and widespread liposomal formulation L0 (55 mol-% EPC and 45 mol-% cholesterol) with limited cargo release.[34] As expected, CHEMS increased retention but decreased release (compare Figure 4A with minimum 80 % and Figure 5A).

Two candidates, L6c and L14c, exhibited poor performance upon CHEMS additions. L6c, primarily composed of stabilizing lipid DPPC, showed minimal cargo retention after 4 h incubation at 37 °C (red boxes in Figure 5A).[35] While CHEMS improved the long-term cargo retention of L14c to 76 %, this value was the weakest among the candidates. Increasing CHEMS from 5 to 10 mol-% did not significantly change retention, but lowered release below 50 % (data not shown).

In contrast, adding 5 mol-% CHEMS in L2c and L15c considerably increased retention above the 90 % while maintaining release above 50 %. For L11c, 5 mol-% CHEMS was

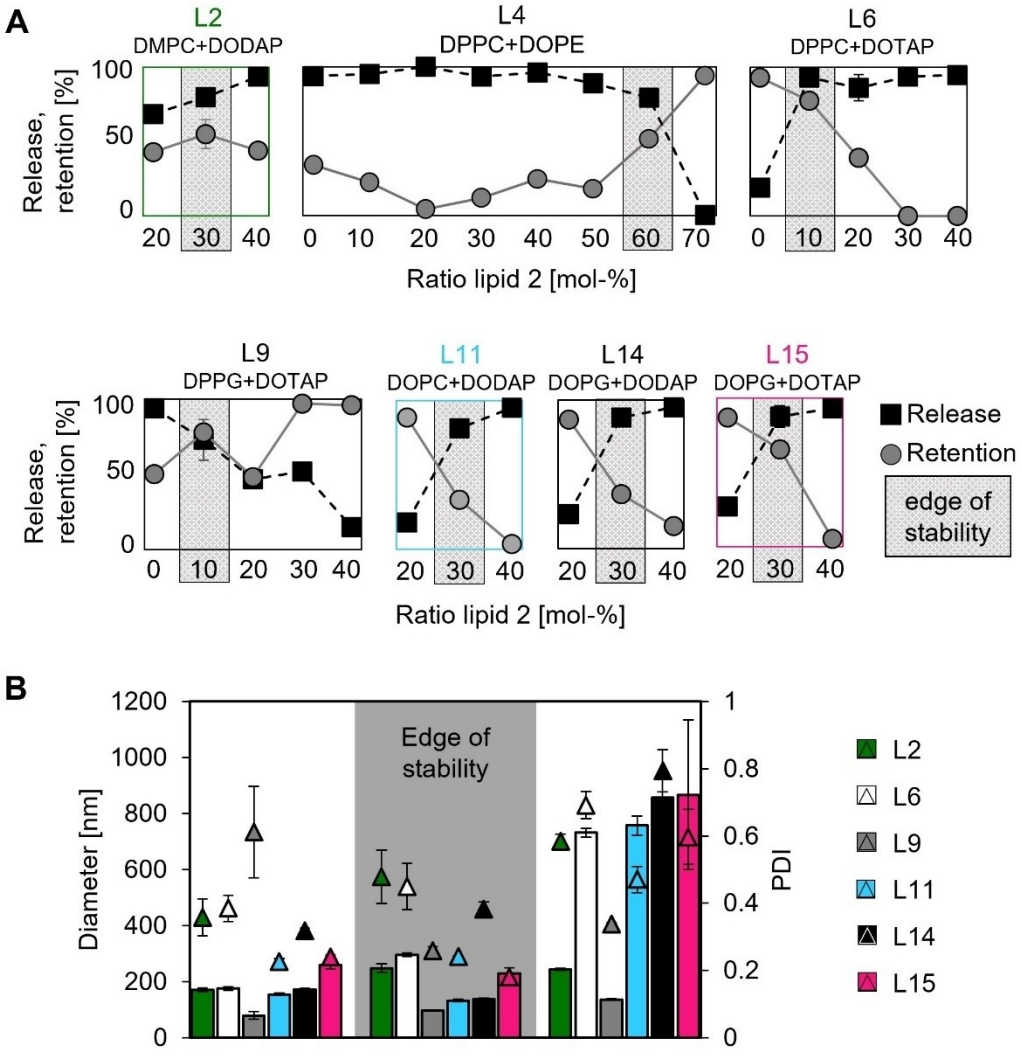

Figure 4. Identification of lipid ratios with increasing modifying lipid that showed high release of SRb at acidic pH and body temperature and corresponding diameter and PDI. **A**: Release (4 h at pH 5.5, 37 °C) and retention of increasing modifying lipid content (n = 3 of sample on edge of stability, n = 1 for sample next to it). Centered are the liposomes considered at "the edge of stability" (grey) with a release above 80% that in addition showed the highest cargo retention (1 week at pH 7.4, 5 °C) within the corresponding composition. Performance drops in cargo release and retention are apparent for liposomes left and right of "the edge of stability", respectively. **B**: Physicochemical parameters with increasing mol-% of lipid 2 obtained from dynamic light scattering (n = 3). Candidate liposomes L2, L11, L14 and L15 were prepared with 20, 30 and 40 mol-% DODAP & DOTAP, respectively, while L6 and L9 was prepared with 0, 10 and 20 mol-% DOTAP. Destabilized liposomes at higher mol-% stand out by high values for diameter (bars) and PDI (triangles), supporting the classification of liposomes at 30 (10) mol-% lipid 2 as "the edge of stability". Error bars indicate standard deviation from three individual liposome preparations. Lead candidates found in Section 2.3.2. are highlighted in color.

insufficient to raise cargo retention from 33% (Figure 4A, Section 2.3.1.) to above 90%, but 10 mol-% CHEMS achieved this target. Consistent with the "molecular plug" effect, we set thresholds of minimum 50% release and 90% retention, after one week of storage for one week and incubation for 4 h at 37 °C. Three candidates (L2c, L11c and L15c) met these criteria (Figure 5A), whose final lipid compositions shown in Figure 5B.

We recapitulated the pH-responsive effect of CHEMS with different cargoes by comparing pH-induced release between liposomes containing either cholesterol or CHEMS (Figure S6), supporting the working hypothesis of using CHEMS *versus* unmodified cholesterol for pH-responsive liposomal drug delivery.

2.3.3. Effect of Serum

Because blood components can affect overall vesicle stability, e.g. by lipid extraction of steroid scaffold lipids, retention and release parameters of the L2c, L11c and L15c were again determined after incubation in full human serum for 4 h at 37 °C (Figure 5C). Indeed, serum incubation lead to a 15–30% drop in retention values after 4 h at 37 °C, although the remaining cargo retention was deemed acceptable for further characterization. Varying the CHEMS content did not improve cargo retention in the presence of human serum (Figure S7).

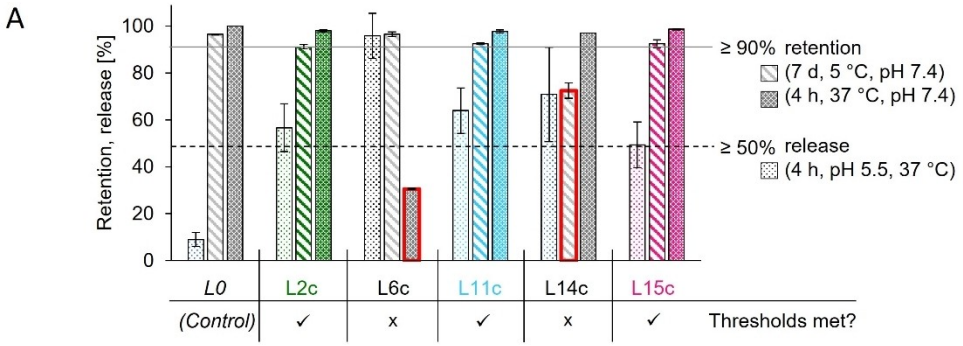

B

Liposome ID	Lipids 1 : 2	Mol-% 1 : 2	Liposome ID	Lipids 1:2	Mol-% 1:2
/	/	/	(L0)	(EPC : CHOL)	(55 : 45)
L2e	DMPC : DODAP	70 : 30	L2c	DMPC : DODAP : CHEMS	66.5 : 28.5 : 5
L11e	DOPC : DODAP	70 : 30	L11c	DOPC : DODAP : CHEMS	63 : 27 : 10
L15e	DOPG : DOTAP	70 : 30	L15c	DOPG : DOTAP : CHEMS	66.5 : 28.5 : 5

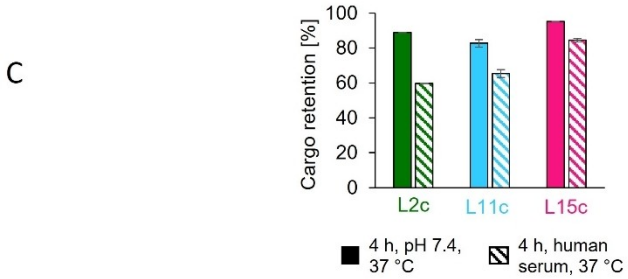

Figure 5. Liposome refinement by incorporation of cholesterylhemisuccinate. **A**: Percentage of cargo release (SRb) and retention for conventional liposome L0 and candidate liposomes L2c, L6c, L15c and L15c with 5 mol-% and L11c with 10 mol-% CHEMS incorporated (n = 3). The dotted lines define the release threshold of at least 50 % and the retention threshold of minimum 90 %. Note that the control liposome L0 showed only little pH-dependent release. Error bars indicate standard deviation from at least three individual liposome preparations. **B**: Lipid compositions and ratios of candidate liposomes with and without CHEMS and control liposome L0 with cholesterol. **C**: Influence of human serum on cargo retention for lead candidate liposomes after incubation for 4 h at 37 °C in the presence or absence of full human serum (n = 3). Lead candidates found are highlighted in color.

2.3.4. Varying the Molecular Cargo

Properties of the lead candidates L2c, L11c and L15c were also investigated with alternative model cargos of comparable molecular weight, namely calcein (Figure S5) and doxorubicin (DXR) (Figure 6).

DLS reported liposome diameters of about 150 to 250 nm, with PDIs below 0.3, regardless of the type of cargo (Figure 6A). After storage at 5 °C for 4 months, L11c and L15c showed no significant changes in size, zeta potentials and PDIs, while L2c showed a higher PDI and an increase in zeta potential, indicating a destabilization that might potentially be related to protonation (Figure 6B).

Acidic incubation at pH 5.5 and 37 °C for 4 h led to a slight decrease in size and an increase in PDI, as observed by DLS (Figure 6B). The zeta potentials of the liposomes L2c and L11c shifted to positive upon acidification, while the zeta potential of L15c increased only slightly and remained negative. The obtained data suggests an acid induced release mechanism due to an increased membrane permeability, rather than liposome aggregation, which would have resulted in a size increase.[20] Transmission electron microscopy (TEM) pictures of all candidates as well as a size comparison before and after cargo release are provided in Figure S8.

2.4. Intracellular Cargo Delivery (Stage 3)

The next stage comprised the *in vitro* validation of liposomal formulations using human melanoma cells (UKRV-Mel-15a) and human monocyte-derived macrophages. We took advantage of doxorubicin hydrochloride as model cargo since its DNA-binding ability and the correlated fluorescence are enabling features for the discrimination between total DXR and DXR released inside the cell and thereby the verification of *in vitro* release from different liposomal formulations.

2.4.1. Toxicity Assay

Empty liposomes showed acceptable toxicity after 72 h in both cell types, with the lowest viability being ~65 % in melanoma cells, measured in a resazurin assay (Figure 7, plain bars). Empty L2c, L11c and L15c showed cytotoxicity comparable to, or

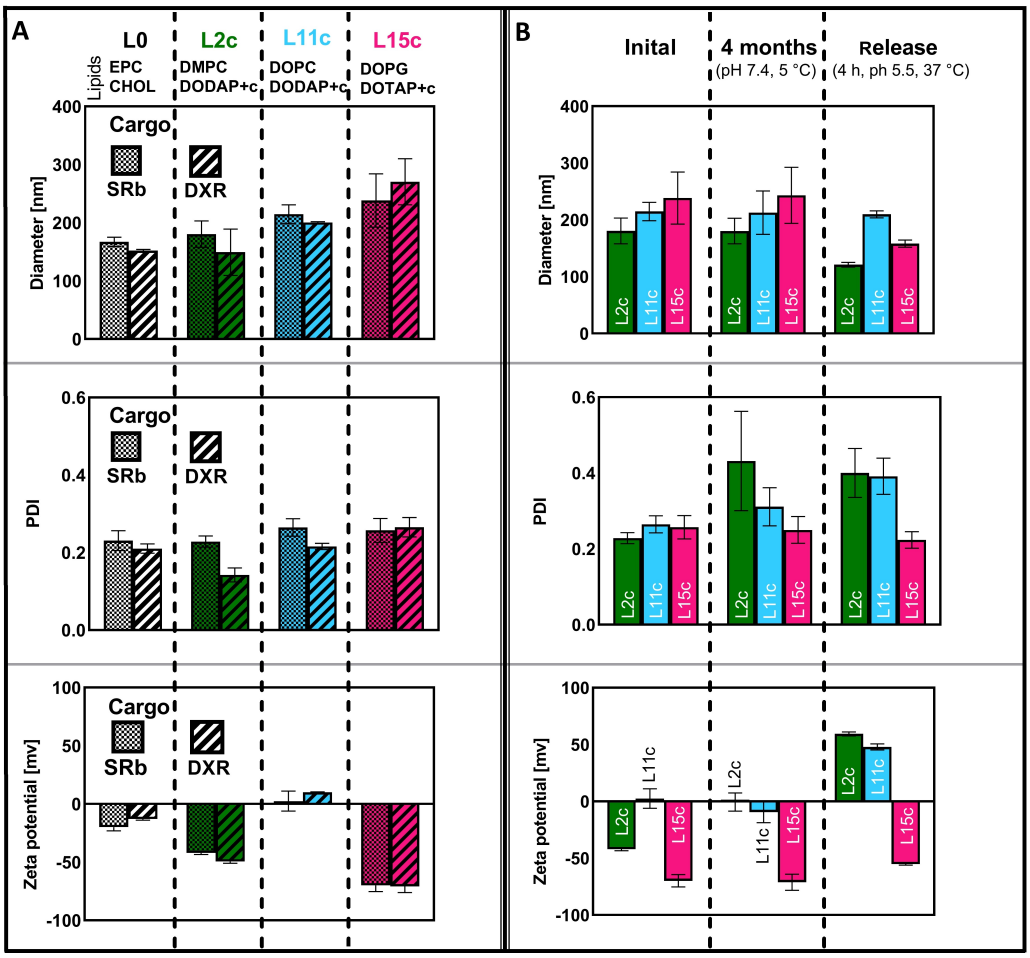

Figure 6. Physicochemical characterization of liposomes by dynamic light scattering. **A**: Diameters, PDIs and zeta potentials of lead candidates L2c, L11c and L15c and control L0 after encapsulation of SRb (checkered bars) or DXR (dashed bars) (n = 3). **B**: Diameters, PDIs and zeta potentials of lead candidates on 1 day or 4 months after preparation (stored at pH 7.4 and 5 °C) and after incubation under release conditions (4 h at pH 5.5 and 37 °C) (n = 3). Depicted, as diameter is the calculated z-average. Error bars indicate standard deviation from three individual liposome preparations.

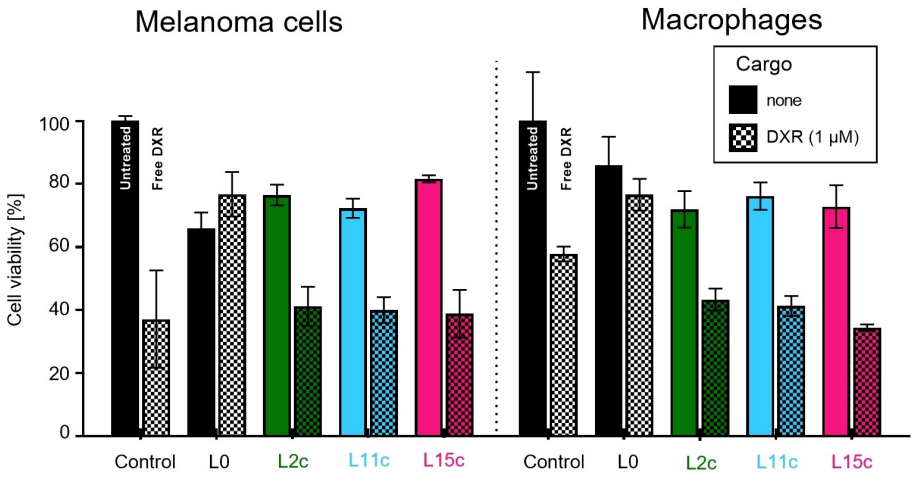

Figure 7. Resazurin assay to determine liposome toxicity after 72 h. Reduction of resazurin to resorufin was used as an indicator for cell viability. Human melanoma (UKRV-Mel-15a) cells and human monocyte-derived macrophages were incubated for 72 h with 1 µM free DXR as positive control, the conventional liposome L0 and the three lead candidates L2c, L11c and L15c all containing DXR equal to 1 µM (checkered bars) or no cargo as control group (plain bars) (n = 9, from 3 independent experiments). Results were normalized to untreated cells.

slightly better than, the control liposome (L0) which is widely regarded as non-toxic (shown in *in vivo* studies[36]).

1 μM DXR-loaded candidate liposome treatment (Figure 7, checkered bars) exhibited toxicity equivalent to 1 μM free DXR treatment in melanoma (~40% viability), and even stronger toxicity than free DXR in macrophages. Toxicity of DXR-loaded lead candidates was ~40% higher compared to the conventional liposome (L0) in both cell types. Together, these findings indicate a successful cargo release in lead candidates. Cell viability after 24 h treatment showed comparable results (Figure S9), although cell viability of DXR containing samples was overall higher due to a shorter incubation period.

2.4.2. Cellular Uptake and Cargo Release Assessed by Flow Cytometry

To assess uptake and intracellular DXR release of liposomes inside the cells, the overall fluorescent signal of DXR per single cell was monitored using flow cytometry.

Melanoma cells (left) showed lower fluorescence signals after 4 h (Figure 8, plain bars), compared to macrophages (right). Also in melanoma cells, candidate liposomes caused fluorescence intensity comparable to free DXR, indicating DXR release, in contrast to control liposome L0. In macrophages, the whole cell fluorescence for candidate liposomes was around three times higher than for L0, but did not reach the level of free DXR. 30 minutes incubation showed comparable results, indicating uptake and accumulation of DXR in all samples, albeit lowest for L0 (Figure S10). Release of DXR from liposomes resulted in fluorescence increase through unquenching, while DNA intercalation decreases fluorescence.[37] Therefore, after a first rough estimation of DXR release from liposomes inside the cells by flow cytometry, we followed up with spatial investigation of different cellular compartments by confocal microscopy.

2.4.3. Model Cargo Accumulation in the Nucleus

Confocal microscopy was used to quantify DXR fluorescence in the nucleus, as DXR intercalates into nuclear DNA only after release from liposomes and cellular organelles, such as endosomes. Nuclei were counterstained with Hoechst 33258. To minimize fluorescence crosstalk, plasma membrane labeling was omitted during these experiments. However, in control experiments where membranes were labeled, we observed that the vast majority of membrane labeled (DiD) liposomes had been taken up by the cell rather than adhering to the outside after sample preparation (Figure S11) and that liposomes did not seem to be able to cross the nuclear membrane. Consistent with the investigations above (2.3.3.), there was no evidence that serum contained in cell culture media (10%) might destabilize liposomes prior cellular uptake, since intact liposomes were visible in confocal microscopy images after 4 h, and no staining of the cellular membrane with liposomal membrane dye DiD was observed.

DXR accumulation in the cell nuclei was quantified, and the results shown in Figure 8 (checkered bars) confirm the conclusions drawn from the flow cytometer analyses: Macrophages displayed higher DXR fluorescence compared to melanoma cells. L0 liposomes showed decreased cargo release compared to L2c, L11c and L15c after 4 h. DXR released from pH-responsive liposomes accumulates as fast as free DXR in the nucleus and reaches the same levels. Data obtained after 30 min of incubation showed the same trends (Figure S10).

Although transfer of lipophilic fluorescent probes, such as DiD, between intact membranes was reported to be

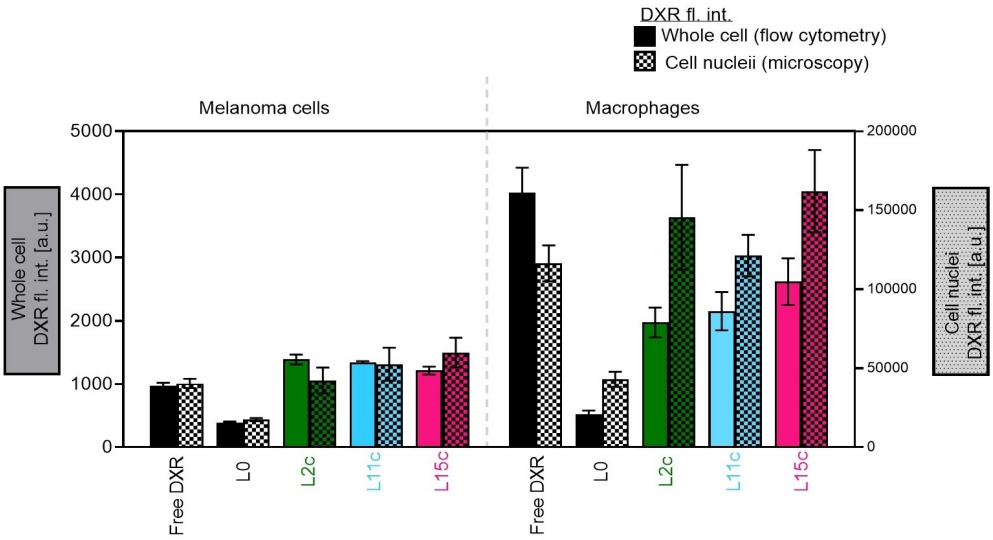

Figure 8. Determination of DXR fluorescence in whole cells by flow cytometry and in cell nuclei by confocal laser microscopy. Liposomal and free DXR fluorescence (dashed bars, left y-axis) in live cells was measured by flow cytometry (n = 11 from 3 independent experiments). DXR fluorescence of nuclei after DXR release from liposomes was measured by confocal microscopy (checkered bars, right y-axis) (n = 3, from 3 independent experiments). UKRV-Mel-15a cells (left) and human monocyte-derived macrophages (right) were incubated for 4 h with 1 μM free DXR as positive control, the conventional liposome L0 and the three lead candidates L2c, L11c and L15c all containing DXR equal to 1 μM. Cell nuclei were counterstained using Hoechst 33258.

negligible,[38] we observed lateral diffusion of DiD within the plasma membrane, visible as staining of the entire cell (Figure 9, pictures 2C–E and 4C–E). Of note, this observation applied exclusively to lead formulations L2c, L11c and L15c, but not to the conventional liposome L0. This effect likely resulted from a decomposition or a change in membrane permeability of the pH responsive candidate liposomes or at least from a change in their membrane permeability within the observed 24 h time span.

2.5. *In vivo* Bio Distribution (Stage 4)

We undertook a limited characterization of the *in vivo* distribution of our lead candidates by live imaging after injection into albino black 6 mice. As a simplistic model, we used phosphate buffer as cargo and limited the label to incorporation of DiR, an NIR dye known to stably integrate into liposomal membranes where it fluoresces strongly, whereas its free form does not.[39] Importantly, our objective was to observe stability during circulation reported by DiR. We complemented the analysis with characterization of the general distribution in the body, and determined detailed amounts in liver and spleen. Fluorescence images and intensity data taken 0 h, 3 h and 24 h after tail vein injection showed similar distributions for the candidates compared to L0 in the abdomen area, shown in Figure 10A and B. Worth mentioning is the strong drop in fluorescence intensity of candidate L11c below 50% of the starting value between 3 h and 24 h. Interestingly, the same formulation showed in the earlier measurement (3 h) the highest fluorescence signal for our three candidates. On the other hand, almost no drop in fluorescent intensity could be observed between 3 h and 24 h for L2c.

The comparison of blood samples taken at 3 h and 24 h showed a relatively lower elimination from bloodstream, for L2c, L11c and L15c compared to L0, suggesting increased blood circulation (Figure 10C).

Subsequently, the mice were sacrificed after 24 h, and liver as well as spleen were fluorescence imaged *ex vivo*. As shown in Figure 10E, substantial DiR fluorescence was found in the liver and spleen for all liposomal formulations. Fluorescence intensities in the liver were roughly comparable among formulations (Figure 10G), whereas values for spleen (Figure 10F) showed significant differences, with particularly low values for L2c and L15c relative to L0 and L11c. These results were confirmed by analysis of extracted DiR from organ slices (Figure S12). At the same time, with the highest drop in blood fluorescence for L0, the DiR signal was not significantly stronger in both organs.

As a summary of the *in vivo* analysis we conclude, that "the edge of stability" formulations were distributed in a fashion mostly similar to the conventional inspired liposomes L0. Exceptions of interest include lower accumulation in the spleen and concomitantly lower elimination capability from bloodstream for L2c and L15c.

3. Conclusions

General aspects: The concept presented allows the screening of large numbers of liposomal formulations to identify lipid compositions that position the resulting liposomes properties

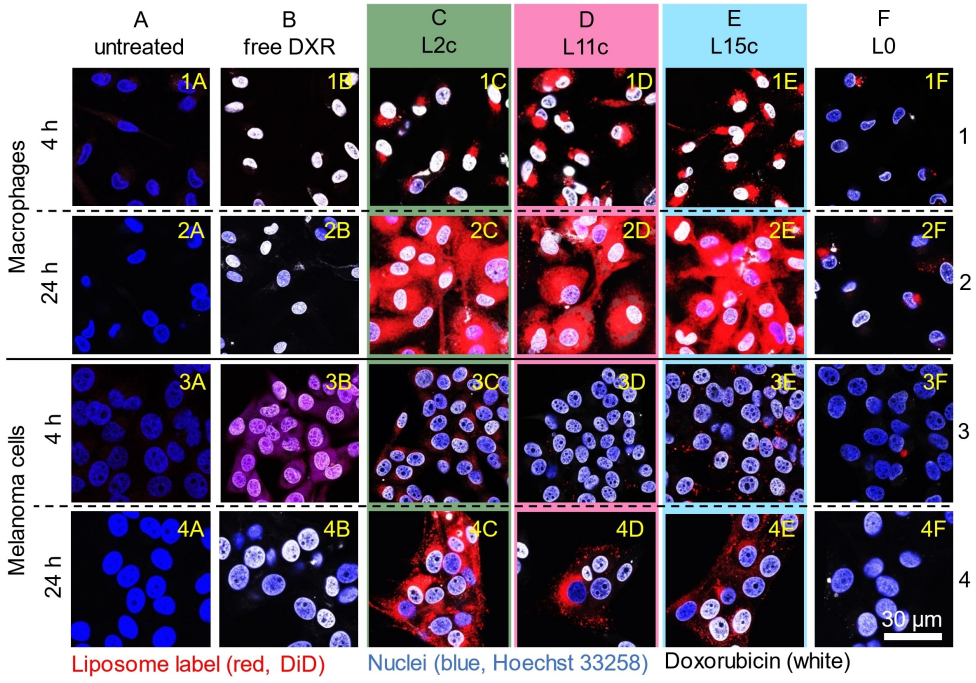

Figure 9. Confocal laser microscopy images of stained nuclei (blue, Hoechst 33258). Human monocyte-derived macrophages (rows 1 and 2) and human melanoma cells (UKRV-Mel-15a, rows 3 and 4) after incubation for 4 and 24 h with free DXR or DXR loaded liposomes (n = 3 from 3 experiments). DXR fluorescence is depicted in white, and liposomes were membrane labeled with membrane dye DiD (red).

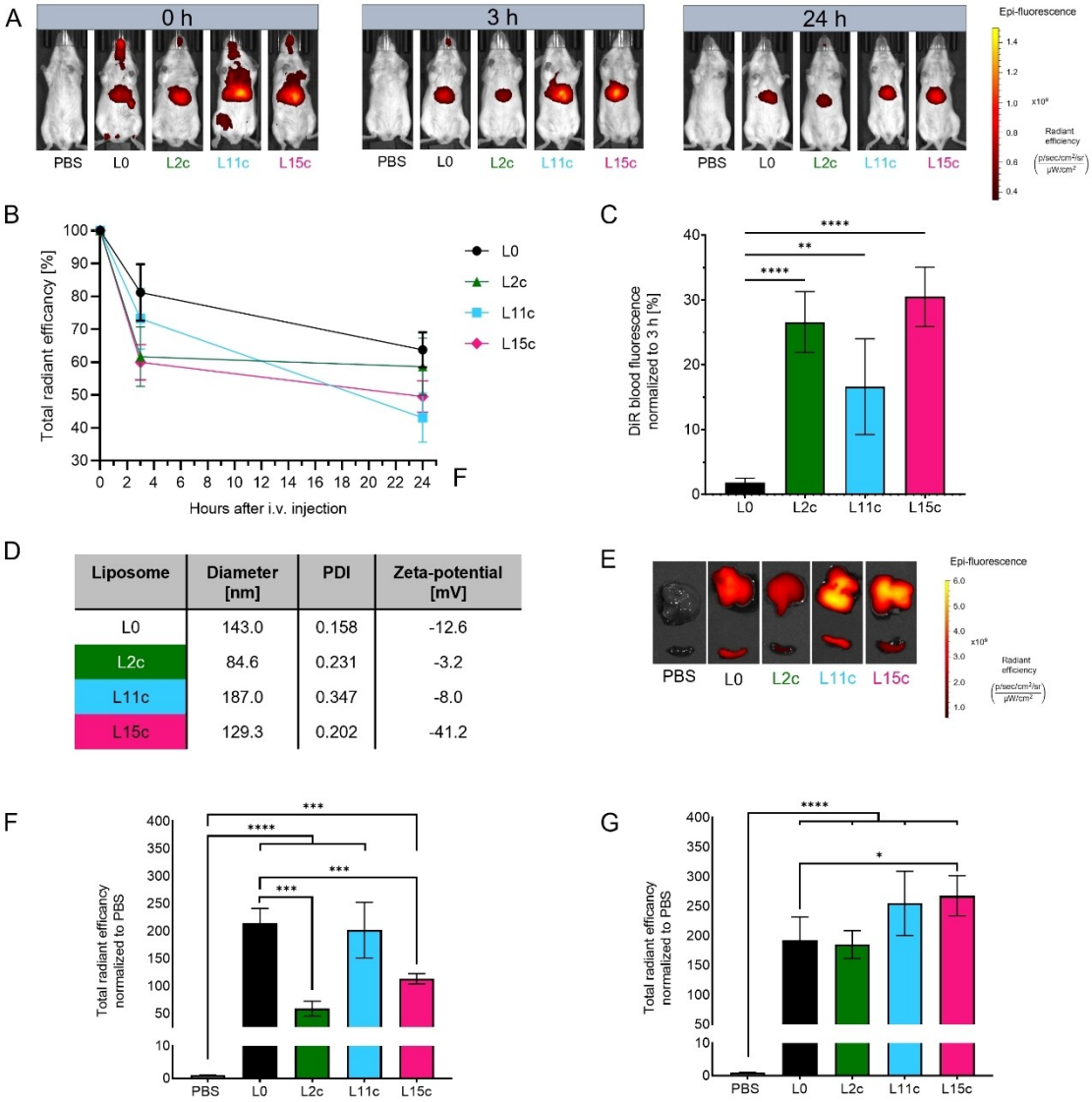

Figure 10. *In vivo* and *ex vivo* analysis after 0 h, 3 h and 24 h after tail vein injection. **A**: Representative DiR fluorescence images of treatment groups. Albino black 6 mice were treated with DiR-labeled lead candidates or PBS as control (L2c, L11c, L15c, L0 (n = 5) at 5 mg/kg bodyweight or only phosphate buffer saline (n = 3)). Signals in the area of mouth and nose are caused by wound care of the animal after injection. **B**: Percent of total radiant efficiency of pH-responsive lipid-nanocarriers in abdomen area displayed for the different timepoints of liposomal candidates and control (n = 5). Total radiant efficiency at 0 h after injection in the abdomen area (lower belly) was set to 100 %. **C**: Blood fluorescence intensity at the experimental end normalized to the 3 h value (phosphate buffer saline group not included) (n = 5). Significances were calculated comparing to L0 (black) via ordinary one-way ANOVA with $r^2 = 0.8622$ for with a 95 % confidence interval. **D**: Table of physicochemical characteristics of liposomal formulations used for biodistribution study. **E**: Fluorescence images of liver (top) and spleen (bottom) taken by *in vivo* imaging 24 h post injection (hpi). Representative images of liver and spleen of treatment groups (L0, L2c, L11c, L15c (n = 5) at 5 mg/kg bodyweight or phosphate buffer saline control (n = 3)) are displayed after normalizing epi-flourescence to the highest values. **F**: Epi-fluorescence from E in spleen (n = 5 for liposomes, n = 3 for control, total of 23 samples) and liver (**G**) (n = 5 for liposomes, n = 3 for control, total of 23 samples) normalized to PBS treatment signal. Significances were calculated to phosphate buffer saline (grey) or L0 (black) via ordinary one-way ANOVA with $r^2 = 0.9091$ (liver) and $r^2 = 0.9060$ (spleen) with a 95 % confidence interval. P-values of ≤ 0.05 are displayed with *, $p \leq 0.01$ is equal to **, while *** and **** show a p-value of ≤ 0.001 and ≤ 0.0001.

at "the edge of stability". This term refers to parameters which were experimentally verified such as shelf-life stability and stimulus-dependent release narrowing the liposomal selection down to 3 out of several hundred possible lipid compositions (binary lipid compositions (Table 2) plus formulations with CHEMS at different mol-%). Our concept has proven itself for hydrophilic small molecules as model cargo, which so far appeared interchangeable among sulforhodamin b, calcein, and doxorubicin, but may have to be rerun for small molecule drugs with higher lipophilicity.

"The edge of stability" is experimentally accessible: The use of the fluorescent dye laurdan into the liposomal membrane enabled the identification of binary lipid compositions that form liposomes at "the edge of stability" showing a sigmoidal curve. While it is clear, that sigmoidal behavior does not *per se* reflect a suitable binary lipid compositions, we employed this method as a rationale first step to narrow down the 168

combinations. This selection criterium significantly impacted the outcome, offering potential for alternative strategies. Our approach appears to work for certain lipids, while others, such as EPC, lack dynamic ranges in this readout, presumably because of inhomogeneity in lipid composition.[40] Implications from these experiments are that (i) certain lipid compositions might escape detection by this assay although being suitable for the task at hand, and (ii) homogenous materials likely show better defined responses to outside stimuli. Other solvatochromic fluorescent membrane probes such as Nile Red or Prodan may help to reveal even more liposomes at "the edge of stability".[41] We further refined the candidate pool from 30 accentuated lipid combinations down to 5 by employing the self-imposed 80% cargo release cut off and simultaneously acceptable stability despite our efforts to minimize rationalism. This logical threshold was implemented with the understanding that stability could be theoretically enhanced in subsequent steps through the molecular plug effect of cholesterol derivates, allowing to prioritize release characteristics at this stage.

Typical liposome destabilization occurred around 40 mol-% lipid 2 (Figure 2, Section 2.2.) while "the edge of stability" was located at lower amounts of destabilizing lipid 2 relative to the inflection point, typically at 30 mol-%. The final lead candidate selection process after implementation of CHEMS necessitated two additional cut-offs, aligning with our primary liposomal design objectives, namely sufficient membrane stability (min. 90%) and efficient payload release (min. 50%, pH 5.5).

Unsuspected pH-responsiveness and helper lipid CHEMS: Most pH-responsive formulations include known pH-sensitive lipids, typically containing ionizable amino groups. L15e (DOPG/DOTAP) exhibited pH-responsiveness without containing ionizable lipids, presumably due to its position at "the edge of stability". Embedment of 5 mol-% CHEMS improved stability for all formulations while maintaining pH-dependent cargo release, but the zeta potential upon acidification was clearly distinct in L15c from those formulations containing ionizable lipids, namely L2c and L11c (both containing DODAP). The zeta potential of L15c remained mostly unchanged at acidic pH, while the latter both showed a positive shift. Diameters of candidate liposomes did not increase upon acidification, suggesting an increased membrane permeability as an acid induced release mechanism. These findings suggest that liposomes at "the edge of stability" might show unsuspected responsiveness to slight changes in pH or temperature.

Increased performance compared to conventional liposome L0: The final candidates showed comparable toxicity to the control liposome L0, which we take as a potential predictor for plausible systemic side effects in *in vivo* applications.[42] DXR-loaded candidates exceeded performance of conventional liposome L0 in terms of cargo release (demonstrated by increased cell death), higher intracellular DXR fluorescence (flow cytometry) and co-localization of DXR in the nuclei (confocal laser microscopy). Quantification of DXR fluorescence in nuclei revealed a three times higher release capability (amount and speed) of candidate liposomes in comparison to L0. We also observed that the liposomal "lead"-formulations distributed *in vivo* in a fashion comparable way compared to L0 with a slight indication of lower elimination from the bloodstream for all three candidates. We see this as a proof-of-principle that should be applicable to a range of lipids, including such that have been in human and have been found non-toxic.

Aspects of intracellular fate: Observations suggest changes in membrane permeability or decomposition of liposomal membranes and even endosomal escape of not only cargo, but also membrane dye, within 24 h for lead candidates, as seen for DiD-labeled liposomes inside the cell after 4 h (without membrane staining, Figure 9). We concluded that negatively charged liposomes might be endocytosed and did not fuse with the cellular membrane, which is in line with reports by Straubinger *et al.*[33a]

Perspectives despite caveats: The presented approach may be applied to liposomes consisting of more than two lipids, allowing for the design and/or development of liposomes with increased complexity and added functionalities influencing stability and cargo release (lipid anchors for stealth-like surface decorations, clickable functionalities for labelling or targeting, stimulus-responsive surface decorations).[24a,43] Future studies are necessary for transition from model-cargo containing lead-candidate liposomes to formulations with dedicated drugs, as the behavior may vary for different cargoes. Also fine-tuning of individual formulations require switching from dual centrifugation to other formulation methods to achieve lower PDI values.

Overall, this study provides a promising approach for identifying liposomal formulations with desirable properties and highlights the potential for further development and optimization.

Author Contributions

Mark Helm: Conceptualization, Methodology, Resources, Writing – Original Draft, Funding acquisition, Writing – review & editing. **Andrea Tuettenberg**: Conceptualization, Methodology, Resources, Writing – Original Draft, Funding acquisition, Writing – review & editing. **Lukas Gleue**: Methodology, Validation, Data Curation, Visualization, Formal analysis, Investigation, Writing – Original Draft, Writing – review & editing. **Barbara Graefen**: Methodology, Validation, Data Curation, Visualization, Formal analysis, Investigation, Writing – Original Draft, Writing – review & editing. **Matthias Voigt**: Conceptualization, Methodology, Validation, Data Curation, Visualization, Formal analysis, Investigation, Writing – Original Draft, Writing – review & editing. **Jonathan Schupp**: Conceptualization, Methodology, Validation, Data Curation, Visualization, Formal analysis, Investigation, Writing – Original Draft, Writing – review & editing. **Dirk Schneider**: Conceptualization, Methodology, Writing – Review & Editing. **Micheal Fichter**: Resources, Writing – Review & Editing, Project administration. **Micheal Kuske**: Resources, Writing – Review & Editing, Project administration. **Volker Mailaender**: Resources, Writing – Review & Editing, Project administration. Final approval of the version to be published was given by all authors and they agreed to be accountable for all aspects of the work.

Acknowledgements

This work was supported by the DFG research center SFB1066, project B14N to MH and AT, Wilhelm-Sander-Foundation (2020.132.2) to AT and Hiege-Stiftung against skin cancer (200504) to AT. DS was supported by the Deutsche Forschungsgemeinschaft (DFG, German Research Foundation, CRC1552 Project Nr 465145163). We thank the imaging core facility of the cell biology unit of Krishnaraj Rajalingam in the PKZI Mainz for providing the Leica SP8 microscope. Open Access funding enabled and organized by Projekt DEAL.

Conflict of Interests

Mark Helm is a consultant for Moderna Inc. Andrea Tuettenberg is the CEO of ActiTrexx GmbH. The other authors report no competing interest.

Data Availability Statement

The data that support the findings of this study are available from the corresponding author upon reasonable request.

Keywords: Screening concept · Dual centrifugation · Intracellular release · Liposomes · Drug delivery

[1] A. Zoghi, K. Khosravi-Darani, A. Omri, *Mini-Rev. Med. Chem.* **2018**, *18*, 324–344, DOI: 10.2174/1389557516666161031120752.
[2] R. Tenchov, R. Bird, A. E. Curtze, Q. Q. Zhou, *ACS Nano* **2021**, *15*, 16982–17015, DOI: 10.1021/acsnano.1c04996.
[3] a) D. Guimaraes, A. Cavaco-Paulo, E. Nogueira, *Int. J. Pharmaceut.* **2021**, *601*, 1–15, DOI: 10.1016/j.ijpharm.2021.120571; b) L. Y. Rizzo, B. Theek, G. Storm, F. Kiessling, T. Lammers, *Curr. Opin. Biotech.* **2013**, *24*, 1159–1166, DOI: 10.1016/j.copbio.2013.02.020.
[4] U. Bulbake, S. Doppalapudi, N. Kommineni, W. Khan, *Pharmaceutics* **2017**, *9*, 1–33, DOI: 10.3390/pharmaceutics9020012.
[5] a) D. C. Drummond, O. Meyer, K. Hong, D. B. Kirpotin, D. Papahadjopoulos, *Pharmacol. Rev.* **1999**, *51*, 691–743; b) D. D. Lasic, D. Needham, *Chem. Rev.* **1995**, *95*, 2601–2628, DOI: 10.1021/cr00040a001; c) M. L. Immordino, F. Dosio, L. Cattel, *Int. J. Nanomedicine* **2006**, *1*, 297–315; d) V. P. Torchilin, V. S. Trubetskoy, K. R. Whiteman, P. Caliceti, P. Ferruti, F. M. Veronese, *J. Pharm. Sci.* **1995**, *84*, 1049–1053, DOI: 10.1002/jps.2600840904.
[6] a) A. Gabizon, R. Shiota, D. Papahadjopoulos, *J. Natl. Cancer Inst.* **1989**, *81*, 1484–1488, DOI: 10.1093/jnci/81.19.1484; b) N. Bertrand, J. C. Leroux, *J. Controlled Release* **2012**, *161*, 152–163, DOI: 10.1016/j.jconrel.2011.09.098.
[7] a) T. Lammers, F. Kiessling, W. E. Hennink, G. Storm, *J. Controlled Release* **2012**, *161*, 175–187, DOI: 10.1016/j.jconrel.2011.09.063; b) V. P. Torchilin, *Handb. Exp. Pharmacol.* **2010**, 3–53, DOI: 10.1007/978-3-642-00477-3_1; c) D. Peer, R. Margalit, *Neoplasia* **2004**, *6*, 343–353, DOI: 10.1593/neo.03460.
[8] a) P. P. Deshpande, S. Biswas, V. P. Torchilin, *Nanomedicine* **2013**, *8*, 1509–1528, DOI: 10.2217/nnm.13.118; b) R. R. Sawant, V. P. Torchilin, *AAPS J.* **2012**, *14*, 303–315, DOI: 10.1208/s12248-012-9330-0; c) Q. Sun, T. Ojha, F. Kiessling, T. Lammers, Y. Shi, *Biomacromolecules* **2017**, *18*, 1449–1459, DOI: 10.1021/acs.biomac.7b00068.
[9] a) S. Simoes, A. Filipe, H. Faneca, M. Mano, N. Penacho, N. Duzgunes, M. P. de Lima, *Expert. Opin. Drug Delivery* **2005**, *2*, 237–254, DOI: 10.1517/17425247.2.2.237; b) N. Duzgunes, C. T. De Ilarduya, S. Simoes, R. I. Zhdanov, K. Konopka, M. C. Pedroso de Lima, *Curr. Med. Chem.* **2003**, *10*, 1213–1220, DOI: 10.2174/0929867033457403.
[10] a) E. Yuba, *J. Mater. Chem. B* **2020**, *8*, 1093–1107, DOI: 10.1039/c9tb02470k; b) L. M. Ickenstein, P. Garidel, *Expert Opin. Drug Delivery* **2019**, *16*, 1205–1226, DOI: 10.1080/17425247.2019.1669558; c) R. R. Sawant, V. P. Torchilin, *Soft Matter* **2010**, *6*, 4026–4044, DOI: 10.1039/b923535n; d) K. Park, *ACS Nano* **2013**, *7*, 7442–7447, DOI: 10.1021/nn404501g; e) T. Ishida, M. J. Kirchmeier, E. H. Moase, S. Zalipsky, T. M. Allen, *Biochim. Biophys. Acta* **2001**, *1515*, 144–158, DOI: 10.1016/s0005-2736(01)00409-6; f) C. Lotter, C. L. Alter, J. S. Bolten, P. Detampel, C. G. Palivan, T. Einfalt, J. Huwyler, *Eur. J. Pharm. Biopharm.* **2022**, *172*, 134–143, DOI: 10.1016/j.ejpb.2022.02.007.
[11] a) A. G. Kohli, P. H. Kierstead, V. J. Venditto, C. L. Walsh, F. C. Szoka, *J. Controlled Release* **2014**, *190*, 274–287, DOI: 10.1016/j.jconrel.2014.04.047; b) S. V. Boddapati, G. G. D'Souza, V. Weissig, in *Methods in Molecular Biology*, *Vol. 605*, 2010/01/15 ed., Springer Protocols, **2010**, pp. 295–303, DOI: 10.1007/978-1-60327-360-2_20; c) J. A. Loureiro, B. Gomes, G. Fricker, I. Cardoso, C. A. Ribeiro, C. Gaiteiro, M. A. Coelho, C. Pereira Mdo, S. Rocha, *Colloids Surf., B* **2015**, *134*, 213–219, DOI: 10.1016/j.colsurfb.2015.06.067; d) S. Bochicchio, B. Dapas, I. Russo, C. Ciacci, O. Piazza, S. De Smedt, E. Pottie, A. A. Barba, G. Grassi, *Int. J. Pharm.* **2017**, *525*, 377–387, DOI: 10.1016/j.ijpharm.2017.02.020; e) H. Ahn, J. H. Park, *Biomater. Res.* **2016**, *20*, 1–6, DOI: 10.1186/s40824-016-0083-1; f) D. Pasarin, A. I. Ghizdareanu, C. E. Enascuta, C. B. Matei, C. Bilbie, L. Paraschiv-Palada, P. A. Veres, *Polymers* **2023**, *15*, DOI: 10.3390/polym15030782.
[12] a) T. Parasassi, G. De Stasio, A. d'Ubaldo, E. Gratton, *Biophys. J.* **1990**, *57*, 1179–1186, DOI: 10.1016/S0006-3495(90)82637-0; b) T. Parasassi, G. De Stasio, G. Ravagnan, R. M. Rusch, E. Gratton, *Biophys. J.* **1991**, *60*, 179–189, DOI: 10.1016/S0006-3495(91)82041-0.
[13] a) G. Bozzuto, A. Molinari, *Int. J. Nanomed.* **2015**, *10*, 975–999, DOI: 10.2147/IJN.S68861; b) E. Evans, D. Needham, *J. Phys. Chem.* **1987**, *91*, 4219–4228, DOI: 10.1021/j100300a003.
[14] E. E. Brumbaugh, C. Huang, *Methods Enzymol.* **1992**, *210*, 521–530, DOI: 10.1016/0076-6879(92)10027-B.
[15] F. M. Harris, K. B. Best, J. D. Bell, *Biochim. Biophys. Acta* **2002**, *1565*, 123–128, DOI: 10.1016/s0005-2736(02)00514-x.
[16] a) G. M'Baye, Y. Mely, G. Duportail, A. S. Klymchenko, *Biophys. J.* **2008**, *95*, 1217–1225, DOI: 10.1529/biophysj.107.127480; b) L. P. Tseng, H. J. Liang, T. W. Chung, Y. Y. Huang, D. Z. Liu, *J. Med. Biol. Eng.* **2007**, *27*, 29–34; c) S. Raffy, J. Teissie, *Biophys. J.* **1999**, *76*, 2072–2080, DOI: 10.1016/S0006-3495(99)77363-7; d) V. A. Tsotas, S. Mourtas, S. G. Antimisiaris, *Drug Delivery* **2007**, *14*, 441–445, DOI: 10.1080/10717540701603530.
[17] a) B. Kneidl, M. Peller, G. Winter, L. H. Lindner, M. Hossann, *Int. J. Nanomedicine* **2014**, *9*, 4387–4398, DOI: 10.2147/IJN.S49297; b) L. H. Lindner, M. E. Eichhorn, H. Eibl, N. Teichert, M. Schmitt-Sody, R. D. Issels, M. Dellian, *Clin. Cancer Res.* **2004**, *10*, 2168–2178, DOI: 10.1158/1078-0432.ccr-03-0035; c) D. Needham, G. Anyarambhatla, G. Kong, M. W. Dewhirst, *Cancer Res.* **2000**, *60*, 1197–1201.
[18] a) V. P. Torchilin, F. Zhou, L. Huang, *J. Liposome Res.* **1993**, 201–255, DOI: 10.3109/08982109309148213; b) S. R. Paliwal, R. Paliwal, S. P. Vyas, *Drug Delivery* **2015**, *22*, 231–242, DOI: 10.3109/10717544.2014.882469; c) H. Karanth, R. S. Murthy, *J. Pharm. Pharmacol.* **2007**, *59*, 469–483, DOI: 10.1211/jpp.59.4.0001.
[19] a) Y. Lee, D. H. Thompson, *WIREs Nanomed. Nanobiotechnol.* **2017**, *9*, 1–76, DOI: 10.1002/wnan.1450; b) P. G. Milhaud, J. P. Bongartz, B. Lebleu, J. R. Philippot, *Drug Delivery* **1996**, *3*, 67–73, DOI: 10.3109/10717549609031175.
[20] H. Ellens, J. Bentz, F. C. Szoka, *Biochemistry* **1984**, *23*, 1532–1538, DOI: 10.1021/bi00302a029.
[21] a) S. Kansiz, Y. M. Elcin, *Adv. Colloid Interface Sci.* **2023**, *317*, 102930, DOI: 10.1016/j.cis.2023.102930; b) M. Ashrafizadeh, M. Delfi, A. Zarrabi, A. Bigham, E. Sharifi, N. Rabiee, A. C. Paiva-Santos, A. P. Kumar, S. C. Tan, K. Hushmandi, J. Ren, E. N. Zare, P. Makvandi, *J. Controlled Release* **2022**, *351*, 50–80, DOI: 10.1016/j.jconrel.2022.08.001; c) E. Yuba, *Polym. J.* **2016**, *48*, 761–771, DOI: 10.1038/pj.2016.31; d) D. C. Drummond, M. Zignani, J. C. Leroux, *Prog. Lipid Res.* **2000**, *39*, 409–460, DOI: 10.1016/S0163-7827(00)00011-4.
[22] a) J. Li, X. L. Wang, T. Zhang, C. L. Wang, Z. J. Huang, X. Luo, Y. H. Deng, *Asian. J. Pharm. Sci.* **2015**, *10*, 81–98, DOI: 10.1016/j.ajps.2014.09.004; b) A. Laouini, C. Jaafar-Maalej, I. Limayen-Blouza, S. Sfar, C. Charcosset, H. Fessi, *J. Colloid Sci. Biotechnol.* **2012**, *1*, 147–168, DOI: 10.1166/jcsb.2012.1020.
[23] a) U. Massing, S. Cicko, V. Ziroli, *J. Controlled Release* **2008**, *125*, 16–24, DOI: 10.1016/j.jconrel.2007.09.010; b) M. Hirsch, V. Ziroli, M. Helm, U. Massing, *J. Controlled Release* **2009**, *135*, 80–88, DOI: 10.1016/j.jconrel.2008.11.029; c) M. Hagedorn, A. Bogershausen, M. Rischer, R. Schubert,

U. Massing, *Int. J. Pharm.* **2017**, *530*, 79–88, DOI: 10.1016/j.ijpharm.2017.07.047.
[24] a) T. Fritz, M. Hirsch, F. C. Richter, S. S. Muller, A. M. Hofmann, K. A. Rusitzka, J. Markl, U. Massing, H. Frey, M. Helm, *Biomacromolecules* **2014**, *15*, 2440–2448, DOI: 10.1021/bm5003027; b) J. K. Koehler, J. Schnur, H. Heerklotz, U. Massing, *Pharmaceutics* **2021**, *13*, DOI: 10.3390/pharmaceutics13122046; c) A. M. Holsæter, K. Wizgird, I. Karlsen, J. F. Hemmingsen, M. Brandl, N. Skalko-Basnet, *Eur. J. Pharm. Sci.* **2022**, *177*, DOI: 10.1016/j.ejps.2022.106267.
[25] U. Massing, S. G. Ingebrigtsen, N. Škalko-Basnet, A. M. Holsæter, InTechOpen **2017**, DOI: 10.5772/intechopen.68523.
[26] S. G. Ong, M. Chitneni, K. S. Lee, L. C. Ming, K. H. Yuen, *Pharmaceutics* **2016**, *8*, 1–12, DOI: 10.3390/pharmaceutics8040036.
[27] N. Kotecha, P. O. Krutzik, J. M. Irish, *Curr. Protoc. Cytom.* **2010**, *Chapter 10*, Unit10 17, DOI: 10.1002/0471142956.cy1017s53.
[28] J. Schindelin, I. Arganda-Carreras, E. Frise, V. Kaynig, M. Longair, T. Pietzsch, S. Preibisch, C. Rueden, S. Saalfeld, B. Schmid, J. Y. Tinevez, D. J. White, V. Hartenstein, K. Eliceiri, P. Tomancak, A. Cardona, *Nat. Methods* **2012**, *9*, 676–682, DOI: 10.1038/nmeth.2019.
[29] a) N. Leber, L. Kaps, M. Aslam, J. Schupp, A. Brose, D. Schaffel, K. Fischer, M. Diken, D. Strand, K. Koynov, A. Tuettenberg, L. Nuhn, R. Zentel, D. Schuppan, *J. Controlled Release* **2017**, *248*, 10–23, DOI: 10.1016/j.jconrel.2016.12.006; b) L. Kaps, L. Nuhn, M. Aslam, A. Brose, F. Foerster, S. Rosigkeit, P. Renz, R. Heck, Y. O. Kim, I. Lieberwirth, D. Schuppan, R. Zentel, *Adv. Healthcare Mater.* **2015**, *4*, 2809–2815, DOI: 10.1002/adhm.201500826.
[30] a) M. J. Sheffield, B. L. Baker, D. Li, N. L. Owen, M. L. Baker, J. D. Bell, *Biochemistry* **1995**, *34*, 7796–7806, DOI: 10.1021/bi00024a003; b) R. Hennig, J. Heidrich, M. Saur, L. Schmuser, S. J. Roeters, N. Hellmann, S. Woutersen, M. Bonn, T. Weidner, J. Markl, D. Schneider, *Nat. Commun.* **2015**, *6*, 1–10, DOI: 10.1038/ncomms8018.
[31] D. Marsh, *Biophys. J.* **2012**, *102*, 1079–1087, DOI: 10.1016/j.bpj.2012.01.049.
[32] F. Vult von Steyern, J. O. Josefsson, S. Tagerud, *J. Histochem. Cytochem.* **1996**, *44*, 267–274, DOI: 10.1177/44.3.8648087.
[33] a) R. M. Straubinger, K. Hong, D. S. Friend, D. Papahadjopoulos, *Cell* **1983**, *32*, 1069–1079, DOI: 10.1016/0092-8674(83)90291-x; b) S. Ohkuma, B. Poole, *Proc. Natl. Acad. Sci. U. S. A.* **1978**, *75*, 3327–3331, DOI: 10.1073/pnas.75.7.3327; c) N. Duzgunes, S. Nir, *Adv. Drug Delivery Rev.* **1999**, *40*, 3–18, DOI: 10.1016/s0169-409x(99)00037-x.
[34] a) E. L.-C. Beltrán-Gracia, A. Higuera-Ciapara, J. B. Velázquez-Fernández, A. A. Vallejo-Cardona, *Cancer Nanotechnol.* **2019**, *10*, 1–40, DOI: 10.1186/s12645-019-0055-y; b) M. B. Bally, R. Nayar, D. Masin, P. R. Cullis, L. D. Mayer, *Cancer Chemother. Pharmacol.* **1990**, *27*, 13–19, DOI: 10.1007/BF00689270; c) L. D. Mayer, L. C. Tai, D. S. Ko, D. Masin, R. S. Ginsberg, P. R. Cullis, M. B. Bally, *Cancer Res.* **1989**, *49*, 5922–5930; d) C. Weber, M. Voigt, J. Simon, A. K. Danner, H. Frey, V. Mailander, M. Helm, S. Morsbach, K. Landfester, *Biomacromolecules* **2019**, *20*, 2989–2999, DOI: 10.1021/acs.biomac.9b00539; e) J. K. Koehler, J. Schnur, H. Heerklotz, U. Massing, *Pharmaceutics* **2021**, *13*, 1–16, DOI: 10.3390/pharmaceutics13122046; f) J. K. Koehler, L. Gedda, L. Wurster, J. Schnur, K. Edwards, H. Heerklotz, U. Massing, *Pharmaceutics* **2023**, *15*, 1–21, DOI: 10.3390/pharmaceutics15020706; g) M. Rozencweig, R. H. Goldfarb, S. Forenza, *United States Patent, Vol. B2*, Sopherion Therapeutics, LLC, East Brunswick, NJ (US) United States, **2011**.
[35] T. Ta, T. M. Porter, *J. Control Release* **2013**, *169*, 112–125, DOI: 10.1016/j.jconrel.2013.03.036.
[36] P. M. Kanter, G. A. Bullard, F. G. Pilkiewicz, L. D. Mayer, P. R. Cullis, Z. P. Pavelic, *In Vivo* **1993**, *7*, 85–95.
[37] R. Hajian, N. Shams, M. Mohagheghian, *J. Brazil Chem. Soc.* **2009**, *20*, 1399–1405, DOI: 10.1590/S0103-50532009000800003.
[38] D. E. Wolf, *Biochemistry* **1985**, *24*, 582–586, DOI: 10.1021/bi00324a006.
[39] a) H. Cho, G. L. Indig, J. Weichert, H. C. Shin, G. S. Kwon, *Nanomedicine* **2012**, *8*, 228–236, DOI: 10.1016/j.nano.2011.06.009; b) L. Gleue, J. Schupp, N. Zimmer, E. Becker, H. Frey, A. Tuettenberg, M. Helm, *Cells* **2020**, *9*, 1–13, DOI: 10.3390/cells9102213.
[40] Y. Y. Zhao, Y. Xiong, J. M. Curtis, *J. Chromatogr. A* **2011**, *1218*, 5470–5479, DOI: 10.1016/j.chroma.2011.06.025.
[41] A. S. Klymchenko, *Acc. Chem. Res.* **2017**, *50*, 366–375, DOI: 10.1021/acs.accounts.6b00517.
[42] a) K. B. Knudsen, H. Northeved, P. E. Kumar, A. Permin, T. Gjetting, T. L. Andresen, S. Larsen, K. M. Wegener, J. Lykkesfeldt, K. Jantzen, S. Loft, P. Moller, M. Roursgaard, *Nanomedicine* **2015**, *11*, 467–477, DOI: 10.1016/j.nano.2014.08.004; b) A. Sharma, S. V. Madhunapantula, G. P. Robertson, *Expert Opin. Drug Metab. Toxicol.* **2012**, *8*, 47–69, DOI: 10.1517/17425255.2012.637916.
[43] T. Fritz, M. Voigt, M. Worm, I. Negwer, S. S. Muller, K. Kettenbach, T. L. Ross, F. Roesch, K. Koynov, H. Frey, M. Helm, *Chem. Eur. J.* **2016**, *22*, 11578–11582, DOI: 10.1002/chem.201602758.

Manuscript received: August 19, 2024
Revised manuscript received: September 20, 2024
Accepted manuscript online: September 27, 2024
Version of record online: November 12, 2024